

NASA TECHNICAL NOTE



NASA TN D-3854

C.1

NASA TN D-3854

LOAN COPY: REPLY
AFWL (WLIL-2)
KIRTLAND AFB, NM

0130656



TECH LIBRARY KAFB, NM

A DESIGN METHOD FOR AN OPTIMAL ATTITUDE REGULATOR FOR A SPINNING SPACE STATION

by Paul S. Rempfer

Langley Research Center

Langley Station, Hampton, Va.





0130656

A DESIGN METHOD FOR AN OPTIMAL ATTITUDE REGULATOR
FOR A SPINNING SPACE STATION

By Paul S. Rempfer

Langley Research Center
Langley Station, Hampton, Va.

NATIONAL AERONAUTICS AND SPACE ADMINISTRATION

For sale by the Clearinghouse for Federal Scientific and Technical Information
Springfield, Virginia 22151 - Price \$2.00

A DESIGN METHOD FOR AN OPTIMAL ATTITUDE REGULATOR FOR A SPINNING SPACE STATION

By Paul S. Rempfer
Langley Research Center

SUMMARY

A study was made to show how a method in optimal control could be used in the design of a linear-feedback attitude regulator for a spinning space station. The design method is for linear systems, and the regulator, operating cyclically, minimizes a final error and uses a fixed amount of control effort in each cycle of operation.

The resulting optimal feedback gains for the optimal regulator are computed and presented. The gains are time-varying and complex. For this reason a suboptimal regulator with less complex time-varying gains is designed on the basis of the optimal system. In addition, for comparison purposes, a standard constant-gain regulator is designed. Digital simulations of all three regulators are presented. It is shown that the two time-varying-gain regulators require a significantly smaller peak control torque than the constant-gain regulator.

INTRODUCTION

In the future, it may be desirable to place a large manned space station in orbit about the earth in order to carry out various extended orbital missions. In order to provide the occupants with an artificial gravity and to provide some attitude stabilization, the station may be spun about one of its principal axes. In reference 1, an optimal regulator control law for linear systems was derived. The optimal regulator operates cyclically and minimizes a final-error magnitude while using a fixed amount of control energy in each cycle of operation. The method is based on the optimal linear regulator theory of reference 2. The present paper shows how this method could be used in the design of an attitude regulator for a large spinning space station.

SYMBOLS

Measurements for the present investigation were taken in the U.S. Customary System of Units. Equivalent values are indicated parenthetically in the International System (SI).

\tilde{A}	4×4 positive definite symmetric matrix determining relative weighting of state variables in terminal-error criterion function
a	positive scalar design parameter in weighting matrix \tilde{A}
\tilde{B}	4×4 positive definite symmetric matrix determining outer hyperellipsoid
\tilde{D}	4×4 positive definite symmetric matrix determining inner hyperellipsoid
E	fixed value of control effort
\vec{e}	unit vector directed along desired orientation of space-station spin axis
\tilde{F}	4×4 matrix determined by dynamics of spinning space station
\bar{g}	4×1 vector-matrix determined by dynamics of spinning space station
\bar{h}	4×1 vector-matrix of feedback gains
h_1, h_2, h_3, h_4	gains in q , r , α , and β , respectively
I	transverse moment of inertia with $I_Y = I_Z$, slug-foot ² (kilogram-meter ²)
I_X, I_Y, I_Z	moments of inertia about principal station X-, Y-, and Z-axes, respectively, slug-foot ² (kilogram-meter ²)
\tilde{I}	4×4 identity matrix
$\vec{i}, \vec{j}, \vec{k}$	unit vectors along principal X-, Y-, and Z-axes, respectively
J	terminal-error criterion function
J_1, J_2	independent constants of motion for free-spinning space station
l	any positive integer
M	element of matrix \tilde{M}
\tilde{M}	4×4 symmetric matrix determining a constant of motion for free-spinning space station

\tilde{P}	4×4 solution matrix defined by equation (17)
\bar{p}	4×1 adjoint variable vector-matrix
p, q, r	angular velocities about principal X-, Y-, and Z-axes, respectively, radians/second
p_0	positive constant spin rate of space station about X-axis, radians/second
s	Laplace transform variable
t	time, seconds
T	fixed operating time for each cycle, seconds
T_Y	control torque applied about Y-axis, foot-pounds (meter-newtons)
u	normalized control input defined in equation (1b), radians/second ²
V	constant of motion for free-spinning space station
X, Y, Z	principal space-station axes
\tilde{X}	4×4 solution matrix for equations of motion for optimally controlled system, defined by equation (22)
\bar{x}	4×1 state-variable vector-matrix defined in equation (1b)
\bar{x}_0	initial state of spinning space station
α, β	angles defining angular misalignment of space station, radians
λ	positive scalar design parameter arising from control effort constraint
σ	dummy scalar variable of integration
τ	dummy scalar variable, $T - t$
$\tilde{\Phi}$	transition matrix for uncontrolled system

$\vec{\Omega}$	total inertial angular velocity of space station, radians/second
ω	frequency defined in equation (1b), radians/second
$\frac{d}{dt}$	derivative with respect to time

Above a variable, a tilde denotes a 4×4 matrix, a bar denotes a 4×1 vector-matrix, and an arrow denotes a vector. Double subscripts on scalars denote elements of a matrix. A prime denotes the transpose of a matrix, and a minus-one superscript denotes the inverse of a matrix. Superscript o denotes optimal system, superscript s denotes suboptimal system, and superscript c denotes constant-gain system. Subscript \max denotes a maximum value. The symbol \triangleq means "is by definition," and the symbol \equiv means "is identically for all time."

PRELIMINARY REMARKS

A possible configuration for a spinning space station is shown in figure 1, where X , Y , and Z denote the principal station axes. The station is assumed to be spinning about the X -axis with a constant rate p_0 ; hence, X is referred to as the spin axis. The rates about the remaining two axes, Y and Z , are denoted q and r , respectively. The orientation in inertial space of the unit vector \vec{e} is that desired for the spin axis, and α and β measure the misalignment of the station spin axis from \vec{e} . The angle α lies in the $\vec{e}Z$ -plane and the angle β lies in the XY -plane.

The spinning space station represents a neutrally stable system. If it receives an impulsive disturbing torque, its spin axis becomes misaligned and moves so as to sweep out a cone which, in general, is not centered about \vec{e} . In this study, the station is assumed to be continually subject to small disturbances which eventually result in an undesirably large misalignment. The object of the regulator is to correct this misalignment in an efficient manner.

It is desired that the regulator perform its job with the least amount of effort. For this reason, as long as the misalignment is small the regulator takes no action. Only when the misalignment reaches an unacceptable level does the regulator operate. At that time, the regulator acts to reduce both the rates, q and r , and the angles, α and β . The regulator operates for a prescribed amount of time and then shuts down until the persistent disturbances again cause an unacceptable misalignment.

A control torque about the Y -axis of the space station supplies the regulator "muscle." Any torque-producing devices capable of producing continuously varying torque magnitudes, such as control moment gyros or reaction wheels, could be used. Ordinarily,

in the design of a regulator, a constant-gain linear-feedback law would be specified and standard Laplace transform techniques used to find the gains. In this study, however, a theory in optimal control is used to provide time-varying gains in order to reduce the peak magnitude of the torques to a value lower than that required by a constant-gain system. This reduction would ease the demands on the torque-producing device and conceivably could reduce its weight and power requirement.

The optimal regulator and its behavior are discussed herein. Its response is compared with that of a simplified suboptimal regulator and with that of a constant-gain system. All the systems considered are linear, and no control saturation is considered.

ANALYSIS

Design of Optimal Regulator

The equations of motion for the spinning station are derived in appendix A by the method used in reference 3. Since the optimal regulator is most simply studied in vector-matrix notation, the equations of motion are presented in that form as

$$\frac{d\bar{x}}{dt} = \tilde{F}\bar{x} + \bar{g}u \quad (1a)$$

where

$$\left. \begin{aligned} \bar{x} &\triangleq \begin{bmatrix} q \\ r \\ \alpha \\ \beta \end{bmatrix} & \tilde{F} &\triangleq \begin{bmatrix} 0 & -\omega & 0 & 0 \\ \omega & 0 & 0 & 0 \\ -1 & 0 & 0 & p_o \\ 0 & -1 & -p_o & 0 \end{bmatrix} \\ \bar{g} &\triangleq \begin{bmatrix} 1 \\ 0 \\ 0 \\ 0 \end{bmatrix} & u &\triangleq \frac{T_Y}{I} & \omega &\triangleq \left(\frac{I_X}{I} - 1 \right) p_o \end{aligned} \right\} \quad (1b)$$

In equation (1b) T_Y denotes the control torque about the Y-axis, I_X denotes the moment of the inertia about the X-axis, and I denotes the moment of inertia about both the Y- and Z-axes. The values for the parameters used in this study are as follows:

I_X , slug-ft ² (kg-m ²)	1.5×10^7	(2.0337×10^7)
I , slug-ft ² (kg-m ²)	1.0×10^7	(1.3558×10^7)
p_o , rad/sec		0.314

The theory used to design the regulator is presented in reference 1. In the optimal theory the activation criterion for the regulator is dependent not only on the misalignment angles, but on the angular rates as well. Specifically, the activation criterion is a positive definite quadratic function of all the components of the state vector. Thus, the regulator takes action whenever the state has reached some four-dimensional ellipsoid in state space and operates to drive the state toward the origin. As a result, the state is kept within this hyperellipsoid. Each time the regulator is activated it remains in operation for a fixed preset amount of time and then shuts down; thus, there is no need for an inner dead band to shut the regulator off. The equation for the hyperellipsoid is given by the optimal theory; and, although the regulator shutdown is governed by time, the optimal theory also gives the equation for a second hyperellipsoid which is inside the first and to which the state is driven on each operation. The size and shape of both the inner and outer hyperellipsoids are discussed subsequently.

Each time the regulator acts, the control torque is governed by a linear-feedback control law which is optimal in that it minimizes a terminal-error function

$$J = \frac{1}{2} \bar{x}'(T) \tilde{A} \bar{x}(T) \quad (2)$$

where $\tilde{A} = \tilde{A}' > 0$ (i.e., J is positive for any nonzero $\bar{x}(T)$) and where T is the fixed operating time, while using a given amount of control effort

$$E = \frac{1}{2} \int_0^T u^2(t) dt \quad (3)$$

Although the constraint on control effort does not imply a constraint on peak control magnitude, it indirectly causes such a constraint since the control is oscillatory and periodic.

The first step in applying the design technique is to choose the \tilde{A} weighting matrix for the terminal error J . Next the optimal feedback control law is found as a function of certain design parameters available to the designer. The third step is to solve for the equations for the inner and outer hyperellipsoids. These hyperellipsoids are dependent on the same parameters as the control law. Finally the designer chooses the design parameters so that the inner and outer hyperellipsoids satisfy the performance requirements of the regulator. These steps are now followed for the space-station problem.

Choice of weighting matrix \tilde{A} . - It can be shown that since the station is neutrally stable there is a matrix $\tilde{M} = \tilde{M}'$ such that, with no control or disturbance acting, the motion of the station satisfies the condition

$$V \triangleq \frac{1}{2} \bar{x}'(t) \tilde{M} \bar{x}(t) \equiv \text{Constant} \quad (4)$$

Because it satisfies this condition, the quadratic form V is called a constant of motion for the uncontrolled system. If this quadratic form is positive definite, it makes an ideal choice for the terminal-error function J , inasmuch as, when J is minimized and the regulator is shut down, except for small disturbances, J remains at its minimized value. The matrix \tilde{M} is then considered as a choice for \tilde{A} .

The matrix \tilde{M} is easily found by taking the derivative of V and utilizing the equation for the uncontrolled system

$$\frac{d\tilde{x}}{dt} = \tilde{F}\tilde{x} \quad (5)$$

with the result

$$\frac{d}{dt} V = \frac{1}{2} \tilde{x}'(t) [\tilde{F}'\tilde{M} + \tilde{M}\tilde{F}]\tilde{x}(t) \equiv 0 \quad (6)$$

The fact that $\tilde{F}'\tilde{M} + \tilde{M}\tilde{F}$ is symmetric and equation (6) is true for all values of $\tilde{x}(t)$ implies that

$$\tilde{F}'\tilde{M} + \tilde{M}\tilde{F} = 0 \quad (7)$$

This equation is solved in appendix B with the result

$$\tilde{M} = \begin{bmatrix} M_{11} & 0 & 0 & -1 \\ 0 & M_{11} & 1 & 0 \\ 0 & 1 & 1.5p_o & 0 \\ -1 & 0 & 0 & 1.5p_o \end{bmatrix} \quad (8)$$

where the element M_{11} is an arbitrary constant. If the quadratic form V is written out, the result is

$$V = \frac{1}{2} \left\{ M_{11}(q^2 + r^2) + \left[1.5p_o(\alpha^2 + \beta^2) + 2(\alpha r - \beta q) \right] \right\} \quad (9)$$

It should be noted that, since V is a constant of the motion of the uncontrolled system for any value of M_{11} , the functions

$$J_1 \triangleq q^2 + r^2 \quad (10)$$

$$J_2 \triangleq 1.5p_o(\alpha^2 + \beta^2) + 2(\alpha r - \beta q) \quad (11)$$

are independently constants of the uncontrolled-system motion. This fact is used subsequently.

Before \tilde{M} may be used as \tilde{A} in the error function it must be tested for positive definiteness. With a useful theorem in reference 4 it is found that, for all positive a , where

$$a \triangleq 3M_{11}p_0 - 2 > 0 \quad (12)$$

\tilde{M} is positive definite. The parameter a is introduced here in order to simplify results presented subsequently. Since \tilde{M} is positive definite, it may now be used as the \tilde{A} weighting matrix. From equation (2) the terminal-error function may then be written (for any $a > 0$) as

$$J = \frac{1}{2} \left\{ \frac{a+2}{3p_0} (q^2 + r^2) + \left[1.5p_0 (\alpha^2 + \beta^2) + 2(\alpha r - \beta q) \right] \right\} \quad (13)$$

From equation (13) it can be seen that the parameter a weights the relative importance of the rates over the angles in the error function. The parameter a is used subsequently as a design parameter.

Determination of the optimal control law.— First, the adjoint vector \bar{p} , which has the same dimension as \bar{x} (i.e., four), is introduced. The adjoint equations are then written as

$$\left. \begin{aligned} \frac{d\bar{p}}{dt} &= -\tilde{F}'\bar{p} \\ \bar{p}(T) &= \tilde{A}\bar{x}(T) \end{aligned} \right\} \quad (14)$$

The theory presented in reference 1 indicates that the optimal control is of the form

$$u^0(t) = -\frac{1}{\lambda} \bar{g}'\bar{p}(t) \quad (15)$$

where λ is another positive design parameter which arises from specifying the amount of control effort. Substituting the optimal control into equation (1a) results in

$$\left. \begin{aligned} \frac{d\bar{x}}{dt} &= \tilde{F}\bar{x} - \frac{1}{\lambda} \bar{g}\bar{g}'\bar{p} \\ \bar{x}(0) &= \bar{x}_0 \end{aligned} \right\} \quad (16)$$

By solving equation (16) and the adjoint equations together, the optimal control may be found as a function of time alone. However, the optimal control as a function of time alone is an optimal open-loop control and not the optimal closed-loop control law desired. In order to obtain the desired feedback law, \bar{p} is determined in terms of \bar{x} by introducing two solution matrices.

The first solution matrix is for the adjoint equation (14) relating $\bar{p}(t)$ to $\bar{x}(T)$ and is denoted $\tilde{P}(T - t)$. This matrix is 4×4 and each column satisfies the adjoint equation so that

$$\left. \begin{aligned} \frac{d\tilde{P}}{dt}(T - t) &= -\tilde{F}'\tilde{P}(T - t) \\ \tilde{P}(0) &= \tilde{A} \end{aligned} \right\} \quad (17)$$

From the terminal conditions on \bar{p} and the equation linearity, the vector \bar{p} may now be written as

$$\bar{p}(t) = \tilde{P}(T - t)\bar{x}(T) \quad (18)$$

Substituting the vector \bar{p} into equation (16) results in

$$\left. \begin{aligned} \frac{d\bar{x}}{dt} &= \tilde{F}\bar{x} - \frac{1}{\lambda} \tilde{g}\tilde{g}'\tilde{P}(T - t)\bar{x}(T) \\ \bar{x}(0) &= \bar{x}_0 \end{aligned} \right\} \quad (19)$$

This is an equation for the optimally controlled system in terms of its initial and final states.

Let $\tilde{\Phi}(T - t)$ denote the transition matrix for the uncontrolled system so that

$$\left. \begin{aligned} \frac{d\tilde{\Phi}}{dt}(T - t) &= \tilde{F}\tilde{\Phi}(T - t) \\ \tilde{\Phi}(0) &= \tilde{I} \end{aligned} \right\} \quad (20)$$

With $\tilde{\Phi}(T - t)$, the solution to equation (19), written in terms of the final state as the sum of its uncontrolled and controlled response, is

$$\bar{x}(t) = \tilde{\Phi}(T - t)\bar{x}(T) + \frac{1}{\lambda} \int_0^{T-t} \tilde{\Phi}(T - t - \sigma) \tilde{g}\tilde{g}'\tilde{P}(\sigma)\bar{x}(T) d\sigma \quad (21)$$

The $\bar{x}(T)$ is then taken outside the integral and factored out of the two terms to give

$$\bar{x}(t) = \left[\tilde{\Phi}(T - t) + \frac{1}{\lambda} \int_0^{T-t} \tilde{\Phi}(T - t - \sigma) \tilde{g}\tilde{g}'\tilde{P}(\sigma) d\sigma \right] \bar{x}(T) \quad (22)$$

By denoting the quantity within the brackets as $\tilde{X}(T - t)$, the second solution matrix, equation (22) is rewritten

$$\bar{x}(t) = \tilde{X}(T - t)\bar{x}(T) \quad (23)$$

It is noted that although $\tilde{X}(T - t)$ does not satisfy the requirements for being the general transition matrix for the optimally controlled system equations, it is shown in reference 2

to be nonsingular. Thus equation (23) may be solved for $\bar{x}(T)$ as

$$\bar{x}(T) = \tilde{X}^{-1}(T - t)\bar{x}(t) \quad (24)$$

and $\bar{x}(T)$ may then be substituted into equation (18) to give \bar{p} as a function of \bar{x} as desired. The resulting equation is

$$\bar{p}(t) = \tilde{P}(T - t)\tilde{X}^{-1}(T - t)\bar{x}(t) \quad (25)$$

When $\bar{p}(t)$ is used in the optimal open-loop control, the optimal closed-loop control law is found to be

$$u^0(t) = -\frac{1}{\lambda} \bar{g}' \tilde{P}(T - t)\tilde{X}^{-1}(T - t)\bar{x}(t) \quad (26)$$

From this law the vector of time-varying gains may be written as those elements multiplying the elements of $\bar{x}(t)$. This vector is denoted $\bar{h}^0(t)$ and is written in row-vector form as

$$\bar{h}^0(t) = -\frac{1}{\lambda} \bar{g}' \tilde{P}(T - t)\tilde{X}^{-1}(T - t) \quad (27)$$

so that the optimal feedback control law is

$$u^0(t) = h_1^0(t)q + h_2^0(t)r + h_3^0(t)\alpha + h_4^0(t)\beta \quad (28)$$

It now remains to explicitly solve for the solution matrices of the space station. By letting $\tau = T - t$ and taking the Laplace transform of equation (17) with respect to τ and by noting that $\frac{d}{dt} = -\frac{d}{d\tau}$, the resulting equation is

$$s\tilde{P}(s) - \tilde{A} = \tilde{F}'\tilde{P}(s) \quad (29)$$

where s denotes the Laplace variable. This equation is then solved for $\tilde{P}(s)$ to give

$$\tilde{P}(s) = (s\tilde{I} - \tilde{F}')^{-1}\tilde{A} \quad (30)$$

Since $\tilde{P}(T - t)$ is not used alone, but only as $\tilde{P}'(T - t)\bar{g}$, and since \bar{g} has only one non-zero component, the matrix multiplication is carried out before inverting the Laplace transform and thus the inversion is greatly simplified. The result is

$$\tilde{P}'(T - t)\bar{g} = \frac{1}{3p_0} \begin{bmatrix} a \cos 0.5p_0(T - t) + 2 \cos p_0(T - t) \\ a \sin 0.5p_0(T - t) - 2 \sin p_0(T - t) \\ -3p_0 \sin p_0(T - t) \\ -3p_0 \cos p_0(T - t) \end{bmatrix} \quad (31)$$

where a can be defined as in equation (12).

With $\tilde{\mathbf{P}}'(T-t)\tilde{\mathbf{g}}$ known, the expression for $\tilde{\mathbf{X}}(T-t)$ can now be transformed with respect to τ with the result

$$\tilde{\mathbf{X}}(s) = (s\tilde{\mathbf{I}} + \tilde{\mathbf{F}})^{-1} + \frac{1}{\lambda}(s\tilde{\mathbf{I}} + \tilde{\mathbf{F}})^{-1}\tilde{\mathbf{g}}\tilde{\mathbf{g}}'\tilde{\mathbf{P}}(s) \quad (32)$$

where $(s\tilde{\mathbf{I}} + \tilde{\mathbf{F}})^{-1}$ is seen from equation (20) to be $\tilde{\Phi}(s)$. (Again, note that $\frac{d}{dt} = -\frac{d}{d\tau}$.) In order to avoid the laborious Laplace inversion and subsequent matrix inversion, rather than solving for $\tilde{\mathbf{X}}(T-t)$ analytically, the differential equation

$$\left. \begin{aligned} \frac{d\tilde{\mathbf{X}}}{dt}(T-t) &= \tilde{\mathbf{F}}\tilde{\mathbf{X}}(T-t) - \frac{1}{\lambda}\tilde{\mathbf{g}}\tilde{\mathbf{g}}'\tilde{\mathbf{P}}(T-t) \\ \tilde{\mathbf{X}}(0) &= \tilde{\mathbf{I}} \end{aligned} \right\} \quad (33)$$

was integrated and the matrix inverse taken on a digital computer to obtain $\tilde{\mathbf{X}}^{-1}(T-t)$. With the digital solution, the time-varying gains could be found by using specified values for the design parameters a and λ and the operating time T .

Equations for inner and outer hyperellipsoids.- As shown in reference 1, the equation for the inner hyperellipsoid is

$$\bar{\mathbf{x}}'(T)\tilde{\mathbf{D}}\bar{\mathbf{x}}(T) = E \quad (34)$$

where E is the magnitude of the control effort and $\tilde{\mathbf{D}} = \tilde{\mathbf{D}}' > 0$ is a 4×4 matrix found by carrying out the integration

$$\tilde{\mathbf{D}} = \frac{1}{2\lambda^2} \int_0^T \tilde{\mathbf{P}}'(\tau)\tilde{\mathbf{g}}\tilde{\mathbf{g}}'\tilde{\mathbf{P}}(\tau)d\tau \quad (35)$$

Since the elements of $\tilde{\mathbf{P}}'(\tau)\tilde{\mathbf{g}}$ are periodic, the integration is simplified by choosing the operating time

$$T = \frac{2\pi}{0.5p_0} l = 40l \quad (l = 1, 2, 3, \dots) \quad (36)$$

The result is

$$\tilde{\mathbf{D}} = \frac{T}{36\lambda^2 p_0^2} \begin{bmatrix} a^2 + 4 & 0 & 0 & -6p_0 \\ 0 & a^2 + 4 & 6p_0 & 0 \\ 0 & 6p_0 & 9p_0^2 & 0 \\ -6p_0 & 0 & 0 & 9p_0^2 \end{bmatrix} \quad (37)$$

The equation for the inner hyperellipsoid is then written as

$$E = \frac{T}{6\lambda^2 p_0} \left[\frac{a^2 + 4}{6p_0} (q^2 + r^2) + 1.5p_0 (\alpha^2 + \beta^2) + 2(\alpha r - \beta q) \right] \quad (38)$$

The quadratic form on the right side of this equation is a constant of motion of the uncontrolled system since it, like J , is simply a linear combination of J_1 and J_2 . Thus, when the state is deposited on the inner hyperellipsoid, except for the disturbances, it stays there.

As shown in reference 1, the equation for the outer hyperellipsoid is

$$\tilde{x}'(0)\tilde{B}\tilde{x}(0) = E \quad (39)$$

where $\tilde{B} = \tilde{B}' > 0$ and when \tilde{B} is a 4×4 matrix defined by the relation

$$\tilde{B} = \tilde{X}^{-1'}(T)\tilde{D}\tilde{X}^{-1}(T) \quad (40)$$

It can be seen that both hyperellipsoids depend on the control effort E and that the \tilde{D} and \tilde{B} matrices depend upon the design parameters a and λ and the operating time T . Hence, the hyperellipsoids may be shaped and sized with these parameters.

Choice of the design parameters.- The first parameter chosen was the operating time T . In this study, T was chosen independent of hyperellipsoid considerations to be 240 seconds, which was considered a reasonable operating time since nearly the same space station had been satisfactorily controlled in this time by a bang-bang controller in reference 5. The remaining parameters were used to adjust the hyperellipsoids. First, an approximate allowable angular misalignment of 0.1 radian was chosen. Then it was necessary to decide how much this misalignment should be reduced each time the regulator was activated. A reduction factor of 10 was chosen so that the terminal misalignment would be about 0.01 radian. Finally, the allowable magnitude of the terminal rates was chosen by considering reference 5 and finding that a ratio of terminal angle to terminal rate of 3.75 seconds was acceptable. Thus the approximate terminal rates would be $0.01 \text{ rad}/3.75 \text{ sec} = 0.00266 \text{ rad/sec}$. With all these requirements, the design parameters were easily found.

Since an analytic expression for the inner hyperellipsoid (eq. (38)) was available, this hyperellipsoid was considered first. An angle α at the inner hyperellipsoid of less than about 0.01 radian was desired. With equation (38), the point on the inner hyperellipsoid at which α is a maximum could be found with the theory of constrained extremals. Then the parameters could be set so that α would satisfy the requirement exactly. Rather than following this procedure herein, however, the point $\alpha = 0.01$, $\beta = q = r = 0.0$ was chosen to lie on the inner hyperellipsoid for the sake of simplicity. Clearly this

point would not be the point of maximum angular misalignment but it was believed to be acceptable for the present example. Similarly, for simplicity, $q = 0.00266$ rad/sec was chosen to lie on the inner hyperellipsoid when $\alpha = \beta = r = 0$. When these two sets of values were substituted into the equation for the inner hyperellipsoid, the two resulting equations were

$$\frac{(240)(0.01)^2}{4\lambda^2} = E \quad (41)$$

$$\frac{(240)(0.00266)^2(a^2 + 4)}{36p_o^2\lambda^2} = E \quad (42)$$

By substituting the value of p_o , the following solutions were obtained:

$$a = 2.9 \quad (43)$$

$$\lambda = \frac{0.0775}{\sqrt{E}} \quad (44)$$

The outer hyperellipsoid condition was then met by choosing E . Since no analytic expression for the \tilde{B} matrix was available, E was chosen by trial and error on a digital computer. First, a small value of E was guessed. Then λ was determined from equation (44) and was used in equation (33) to solve for $\tilde{X}(T)$. By substituting $\tilde{X}(T)$ into equation (40), the matrix \tilde{B} was computed. This matrix determined the outer hyperellipsoid. Again, for simplicity, rather than using the theory of constrained extremals, the condition that $\alpha = 0.1$, $\beta = q = r = 0.0$ lie on this hyperellipsoid was then checked. Since a small value of E had been chosen, the hyperellipsoid was too small and fell within the checkpoint. The value of E was then successively increased until the check condition was met. This procedure was quite simple and required only four iterations. The result was

$$E = 8.13 \times 10^{-6} \quad (45)$$

Thus, all the parameters were chosen and they completely fixed the two hyperellipsoids and the optimal feedback control law. The characteristics of the hyperellipsoids and the optimal gains are now discussed.

Study of Optimal Regulator

The matrix \tilde{B} was computed to be

$$\tilde{B} = \begin{bmatrix} 7.34 \times 10^{-3} & -1.80 \times 10^{-7} & -1.43 \times 10^{-7} & -1.73 \times 10^{-3} \\ -1.80 \times 10^{-7} & 7.30 \times 10^{-3} & 1.73 \times 10^{-3} & 4.10 \times 10^{-8} \\ -1.43 \times 10^{-7} & 1.72 \times 10^{-3} & 8.12 \times 10^{-4} & 3.25 \times 10^{-8} \\ -1.73 \times 10^{-3} & 4.10 \times 10^{-8} & 3.25 \times 10^{-8} & 8.14 \times 10^{-4} \end{bmatrix} \quad (46)$$

When the quadratic form $\bar{x}'\tilde{B}\bar{x}$ is written out, with terms of the order 10^{-7} or less neglected, an approximate but very close equation for the outer hyperellipsoid may be written as

$$0.00173 \left[4.23(q^2 + r^2) + 1.5p_o(\alpha^2 + \beta^2) + 2(\alpha r - \beta q) \right] = E \quad (47)$$

Like J and the inner-hyperellipsoid quadratic form, this expression is also a constant of the motion of the uncontrolled system since it is simply a linear combination of J_1 and J_2 . Although it is difficult to visualize either hyperellipsoid because they both lie in four-dimensional space, some information may be gained by looking at certain cross sections. (See fig. 2.)

From either of the two hyperellipsoid equations, it can be seen that a cross section in or parallel to the $\alpha\beta$ - or qr -plane is a circle. When either both the rates or both the angles are zero, the circle has its largest radius and encircles the origin as shown in figures 2(a) and 2(b). The three points used to choose the design parameters are shown in these figures. From the equations, it may further be seen that cross sections in or parallel to the $r\alpha$ - or $q\beta$ -plane are ellipses which are tilted because of the cross-product terms. When both β and q or both r and α are zero, the ellipses are at their largest and are centered about zero as shown in figures 2(c) and 2(d). In these figures, it is seen that the approximate angular misalignment requirements are exceeded because of the tilting of the ellipses. Further study of the hyperellipsoid equations shows that the maximum violations of the requirements occur in these cross sections. For the present problem the violations were considered acceptable. It should be pointed out that, if they had not been acceptable, more conservative approximate errors could have been chosen and the design process repeated once or twice with very little additional work. Use of the theory of constrained extremals previously mentioned could also have been made but was considered unnecessary for this study.

The time-varying optimal gains are presented in figure 3. The gains generally increase with time and there is clearly a greater dependence on q and β than on r and α .

Design of Suboptimal Regulator

In applying the optimal regulator, it is necessary to monitor the function $0.00173(4.23J_1 + J_2)$ where J_1 and J_2 are the constants of the uncontrolled motion, which are defined in equations (10) and (11). When this monitored function reaches the value $E = 8.13 \times 10^{-6}$, the state would be on the outer hypersurface, since equation (47) for the outer hyperellipsoid is satisfied, and the control would be turned on. The control law then uses stored values for the time-varying gains and the whole state vector is fed back. This process is complex since it involves storage and many multipliers, and therefore a simplified suboptimal regulator was considered.

Since the gains on α and r for the optimal control were small, they were taken as zero for the suboptimal control. Thus, the dependence on α and r was eliminated. Next, it can be seen in figure 3 that the q gain, although negative, is nearly proportional to the β gain for the entire operation. In the suboptimal control, therefore, the constant of proportionality was estimated and used to give

$$h_1^S = -4.23h_4^S \quad (48)$$

Then the time variation lay all in one gain h_4^S . In order to eliminate the necessity of storing this gain, the following simple time function approximating it was constructed:

$$h_4^S = 0.0037[\exp(0.0085t) - 0.0077t] \quad (49)$$

The nonzero suboptimal gains resulting from the approximations are compared with the optimal gains in figure 4. Thus, the suboptimal control has been simplified to

$$u^S = h_4^S(\beta - 4.23q) \quad (50)$$

Since the dependence of the control on α and r has been eliminated, it is desirable for J_1 and J_2 to be determined without measuring α and r . The need for measuring α and r would then be eliminated completely. A possible method for such a determination of J_1 and J_2 is presented in appendix C, although it was not actually simulated in this study. In all simulations the suboptimal control system was initiated on the outer hyperellipsoid with the same initial conditions as the optimal system. The behavior of the two systems is compared in the section "Results and Discussion."

Constant-Gain Control

In order to compare the optimal and suboptimal regulators with a standard constant-gain regulator which performs the same function, a constant-gain regulator was designed by the use of only q and β feedback as is required for the suboptimal control. It was believed that the ratio of β gain to q gain used in the suboptimal control law was probably a good one and so this ratio was used in the constant-gain system

$$h_1^C = -4.23h_4^C \quad (51)$$

The constant gain h_4^C was then found by trying values for h_4^C , digitally computing the system response, and then comparing the resulting terminal motion with the terminal motion of the suboptimal system. When the terminal motions appeared equivalent, that value which had been used was the gain. The value in the present study was

$$h_4^C = 0.01 \quad (52)$$

The constant-gain feedback control was then

$$u^C = 0.01(\beta - 4.23q) \quad (53)$$

In the next section the performance of this system is compared with that of the other two regulators.

RESULTS AND DISCUSSION

Optimal Regulator

Figures 5 to 7 show the performance of the optimal regulator operating from various points on the outer hyperellipsoid. These points are representative of the initial conditions the regulator might encounter. It is important to notice the constant amplitude of the periodic control variable evident for all three initial conditions. This constant amplitude is a general characteristic of the optimal regulator. Because of this characteristic, the maximum magnitude of control torque which the regulator requires at any time may be estimated. The maximum magnitude occurs when the regulator operates from initial conditions in the $q\beta$ -plane where the straight line of the equation

$$\beta - 4.23q = \text{Constant} \quad (54)$$

just touches the ellipse. The points satisfying this requirement (one of which is the initial condition of fig. 5) are shown in figure 2(d). The estimated maximum magnitude of control torque required is found to be 5200 ft-lbf (7050 m-N).

The constant-amplitude characteristic of the optimal control is responsible for the linear decay envelop of the rates and angles. For the initial conditions in figures 5 to 7, the envelop indicated a time to damp to half amplitude of 130 seconds.

Suboptimal Regulator

Figures 8 to 10 show the performance of the suboptimal regulator operating from the same initial conditions as the optimal regulator in figures 5 to 7. The time histories appear to be the same as for the optimal regulator during about the first 180 seconds. This similarity exists because the suboptimal gains approximate the optimal gains almost exactly for this time period. As the approximation becomes less exact, the suboptimal control drops slightly in amplitude. The result is that the angles and rates left after the suboptimal regulator shuts down are slightly larger than those left by the optimal regulator. The difference, however, is very small. The time to damp to half amplitude is the same as for the optimal regulator – that is, 130 seconds; however, because the suboptimal control amplitude drops off toward the end of each operation, the suboptimal control effort is less than the optimal control effort. For the simulations in this study the value of E used by the suboptimal regulator is from 1 percent to 7 percent lower than that used by the optimal regulator. The dropping off of the control amplitude does not, however, affect the magnitude of the required control torque, which is estimated at 5200 ft-lbf (7050 m-N), the same as for the optimal system.

Constant-Gain Regulator

Figures 11 to 13 show the performance of the constant-gain regulator operating from the same initial conditions as the optimal and suboptimal systems. The behavior of this regulator is the standard constant-gain behavior. The control amplitude drops off as the angles and rates decay and thus an exponential envelop for the variables is formed. It is important to note that, although the terminal rates and angles are comparable to those of the two systems discussed previously, the time to damp to half amplitude is much shorter – 66 seconds. The price that the constant-gain system pays for this time reduction is more control effort. The value of E used by the constant-gain regulator is from 42 percent to 44 percent higher than that used by the optimal regulator. More important, the maximum control-torque magnitude required by the constant-gain regulator is 13 820 ft-lbf (18 737 m-N). (See fig. 11.) This value is 2.7 times the maximum control-torque magnitude required by the optimal or suboptimal regulators. Since only terminal error is of interest, this result indicates that the optimal and suboptimal regulators make much more effective use of a given magnitude of available control torque than does the constant-gain regulator.

CONCLUDING REMARKS

An optimal linear-feedback regulator has been designed for the attitude control of a spinning space station. The optimal regulator employs time-varying gains to make continued use of its available peak control torque. In contrast, a constant-gain system uses its available peak control torque only in the initial phases of its control operation. Thus, the magnitude of the peak control torque that the optimal regulator requires is significantly lower than that required by the constant-gain system. This reduction in torque-magnitude requirement is obtained, however, at the expense of system complexity. For this reason, a suboptimal system, which is much simpler than the optimal system but which has near-optimal performance, has been designed. The suboptimal system is more complex than the constant-gain system, but this complexity may be warranted in a space station where available control torque is at a premium.

Langley Research Center,
National Aeronautics and Space Administration,
Langley Station, Hampton, Va., November 8, 1966,
125-19-04-01-23.

APPENDIX A

VEHICLE DYNAMICS

The rate equations of motion for the spinning vehicle are simply a special case of Euler's dynamical equations (see ref. 6) with the following assumptions employed:

- (1) Symmetric inertia distribution, that is, $I_Y = I_Z = I$
- (2) No component of torques about the X or Z axes
- (3) The space-station moment of inertia about the spin axis satisfies the inequality $I_X > I$.

With these assumptions, Euler's dynamical equations are written as

$$I_X \frac{dp}{dt} = 0 \quad (A1)$$

$$I \frac{dq}{dt} - (I - I_X)p r = T_Y \quad (A2)$$

$$I \frac{dr}{dt} - (I_X - I)p q = 0 \quad (A3)$$

From equation (A1) the spin rate is constant and is denoted p_o . Equations (A2) and (A3) may then be rewritten

$$\frac{dq}{dt} + \omega r = \frac{T_Y}{I} \quad (A4)$$

$$\frac{dr}{dt} - \omega q = 0 \quad (A5)$$

where

$$\omega = \left(\frac{I_X}{I} - 1 \right) p_o \quad (A6)$$

The angle equations are written with the assumption that \vec{e} is fixed in inertial space. With respect to the body axes, \vec{e} then satisfies the equation

$$\frac{d}{dt} \vec{e} + \vec{\Omega} \times \vec{e} = 0 \quad (A7)$$

where

$$\vec{\Omega} = p_o \vec{i} + q \vec{j} + r \vec{k} \quad (A8)$$

APPENDIX A

and \vec{i} , \vec{j} , and \vec{k} are unit vectors along the X, Y, and Z axes, respectively. From figure 1 it may be seen that in the body-axis coordinates the vector \vec{e} is

$$\vec{e} = \cos \alpha \cos \beta \vec{i} + \cos \alpha \sin \beta \vec{j} - \sin \alpha \vec{k} \quad (\text{A9})$$

Equation (A7) is then linearized by assuming that

$$\left. \begin{aligned} \sin \alpha &= \alpha \\ \cos \alpha &= 1 \\ \sin \beta &= \beta \\ \cos \beta &= 1 \end{aligned} \right\} \quad (\text{A10})$$

and that the products $\alpha \frac{d\alpha}{dt}$, $\beta \frac{d\beta}{dt}$, $q\alpha$, and $r\beta$ are small and may be neglected. These assumptions have been shown to be good for vehicles in motion with angular misalignments of less than 15° (see ref. 7). The resulting equations are

$$\frac{d\alpha}{dt} - p_0 \beta = -q \quad (\text{A11})$$

$$\frac{d\beta}{dt} + p_0 \alpha = -r \quad (\text{A12})$$

Equations (A4), (A5), (A11), and (A12) compose the set of equations used in this study.

APPENDIX B

SOLUTION FOR MATRIX \tilde{M}

The equation which must be solved is written

$$\tilde{F}'\tilde{M} + \tilde{M}\tilde{F} = 0 \quad (B1)$$

where $\tilde{M} = \tilde{M}'$. Since \tilde{M} is symmetric, equation (B1) may be rewritten

$$(\tilde{M}\tilde{F})' + \tilde{M}\tilde{F} = 0 \quad (B2)$$

In order to use this equation, \tilde{M} is set up as

$$\tilde{M} = \begin{bmatrix} M_{11} & M_{12} & M_{13} & M_{14} \\ M_{12} & M_{22} & M_{23} & M_{24} \\ M_{13} & M_{23} & M_{33} & M_{34} \\ M_{14} & M_{24} & M_{34} & M_{44} \end{bmatrix} \quad (B3)$$

and multiplied by \tilde{F} to give

$$\tilde{M}\tilde{F} = \begin{bmatrix} \frac{1}{2} p_o M_{12} - M_{13} & -\frac{1}{2} p_o M_{11} - M_{14} & -p_o M_{14} & p_o M_{13} \\ \frac{1}{2} p_o M_{22} - M_{23} & -\frac{1}{2} p_o M_{12} - M_{24} & -p_o M_{24} & p_o M_{23} \\ \frac{1}{2} p_o M_{23} - M_{33} & -\frac{1}{2} p_o M_{13} - M_{34} & -p_o M_{34} & p_o M_{33} \\ \frac{1}{2} p_o M_{24} - M_{34} & -\frac{1}{2} p_o M_{14} - M_{44} & -p_o M_{44} & p_o M_{34} \end{bmatrix} \quad (B4)$$

Then $\tilde{M}\tilde{F}$ is transposed and added to itself term by term to arrive at equation (B2).

In equation (B2) there are 16 algebraic equations, not all independent, which are solved to give \tilde{M} . The result is

$$\tilde{M} = \begin{bmatrix} M_{11} & 0 & 0 & -M_{33}/1.5p_o \\ 0 & M_{11} & M_{33}/1.5p_o & 0 \\ 0 & M_{33}/1.5p_o & M_{33} & 0 \\ -M_{33}/1.5p_o & 0 & 0 & M_{33} \end{bmatrix} \quad (B5)$$

APPENDIX B

where both M_{11} and M_{33} are arbitrary constants. Notice that \tilde{M} may be rewritten as

$$\tilde{M} = M_{33} \begin{bmatrix} M_{11}/M_{33} & 0 & 0 & -1/1.5p_o \\ 0 & M_{11}/M_{33} & 1/1.5p_o & 0 \\ 0 & 1/1.5p_o & 1 & 0 \\ -1/1.5p_o & 0 & 0 & 1 \end{bmatrix} \quad (B6)$$

which shows \tilde{M} to be arbitrary in the "magnitude" M_{33} . The reason is that equation (B1) is homogeneous and thus the magnitude does not reflect any system characteristic. In this study, M_{33} was chosen to be $1.5p_o$ in order to avoid the fractions in \tilde{M} . Thus, the result is

$$\tilde{M} = \begin{bmatrix} M_{11} & 0 & 0 & -1 \\ 0 & M_{11} & 1 & 0 \\ 0 & 1 & 1.5p_o & 0 \\ -1 & 0 & 0 & 1.5p_o \end{bmatrix} \quad (B7)$$

APPENDIX C

METHOD FOR DETERMINING J_1 AND J_2

Since, for the suboptimal system, the dependence of the control on α and r has been eliminated, it is desired that J_1 and J_2 be determined without measurement of α and r . The need for measuring α and r would then be eliminated completely. Such a determination of J_1 and J_2 is possible, but it requires that the disturbance effects be small over any 40-second beat period of the space-station motion. With this requirement, the equations of motion for the uncontrolled system are

$$\frac{dq}{dt} = -0.5p_0 r \quad (C1)$$

$$\frac{dr}{dt} = 0.5p_0 q \quad (C2)$$

$$\frac{d\alpha}{dt} = -q + p_0 \beta \quad (C3)$$

$$\frac{d\beta}{dt} = -r - p_0 \alpha \quad (C4)$$

From equation (C1) it is evident that, when q is a maximum, r is zero so

$$J_1 = q_{\max}^2 \quad (C5)$$

If equation (11) is rewritten as

$$J_2 = \frac{1}{1.5p_0} \left[(1.5p_0 \alpha + r)^2 + (1.5p_0 \beta - q)^2 - J_1 \right] \quad (C6)$$

then, with the equations of the uncontrolled motion, it may be found that

$$\frac{d}{dt} (1.5p_0 \beta - q) = -p_0 (1.5p_0 \alpha + r) \quad (C7)$$

so that the second term within the brackets in equation (C6) is a maximum when the first term within the brackets is zero. The resulting equation is

$$J_2 = \frac{1}{1.5p_0} \left[(1.5p_0 \beta - q)_{\max}^2 - J_1 \right] \quad (C8)$$

The function which must be monitored to determine whether the state has reached the outer hyperellipsoid may then be written in terms of q_{\max} and $(1.5p_0 \beta - q)_{\max}$. Thus the need for α and r sensors in the suboptimal system is eliminated.

REFERENCES

1. Rempfer, Paul S.: An Activation Criterion for Repeated Use of an Optimal Fixed Time Constant Energy Regulator. Conference Record – Twelfth Annual East Coast Conference on Aerospace and Navigational Electronics, IEEE, Oct. 1965, pp. 3.4.5-1 – 3.4.5-5.
2. Kalman, R. E.: Contributions to the Theory of Optimal Control. Bol. Soc. Mat. Mex., vol. 5, 1960, pp. 102-119.
3. Suddath, Jerrold H.; and Carney, Terrance M.: Technique for Synthesis of Constant Linear Dynamical Systems With a Bang-Bang Controller. NASA TR R-200, 1964.
4. Bellman, Richard: Introduction to Matrix Analysis. McGraw-Hill Book Co., Inc., 1960, pp. 72-74.
5. Rempfer, Paul S.; and Suddath, Jerrold H.: Application of a Bang-Bang Control System to Two Spinning Space Vehicles. NASA TN D-2596, 1965.
6. Goldstein, Herbert: Classical Mechanics. Addison-Wesley Pub. Co., Inc. (Reading, Mass.), c.1959.
7. Suddath Jerrold H.: A Theoretical Study of the Angular Motions of Spinning Bodies in Space. NASA TR R-83, 1961.

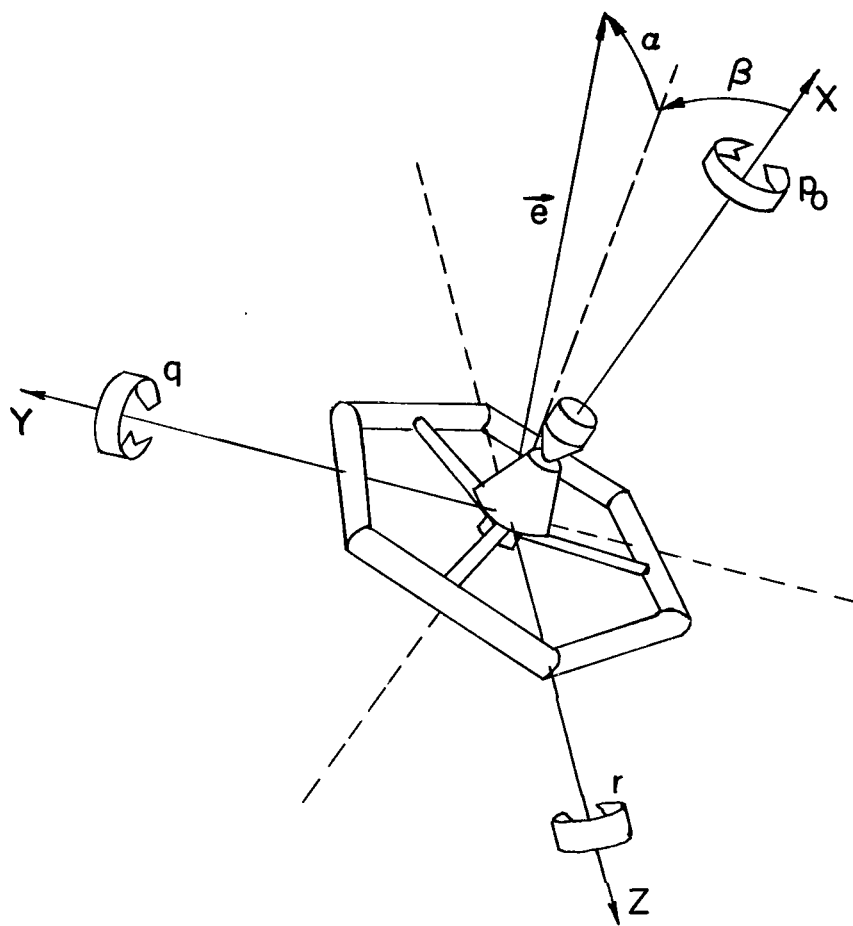
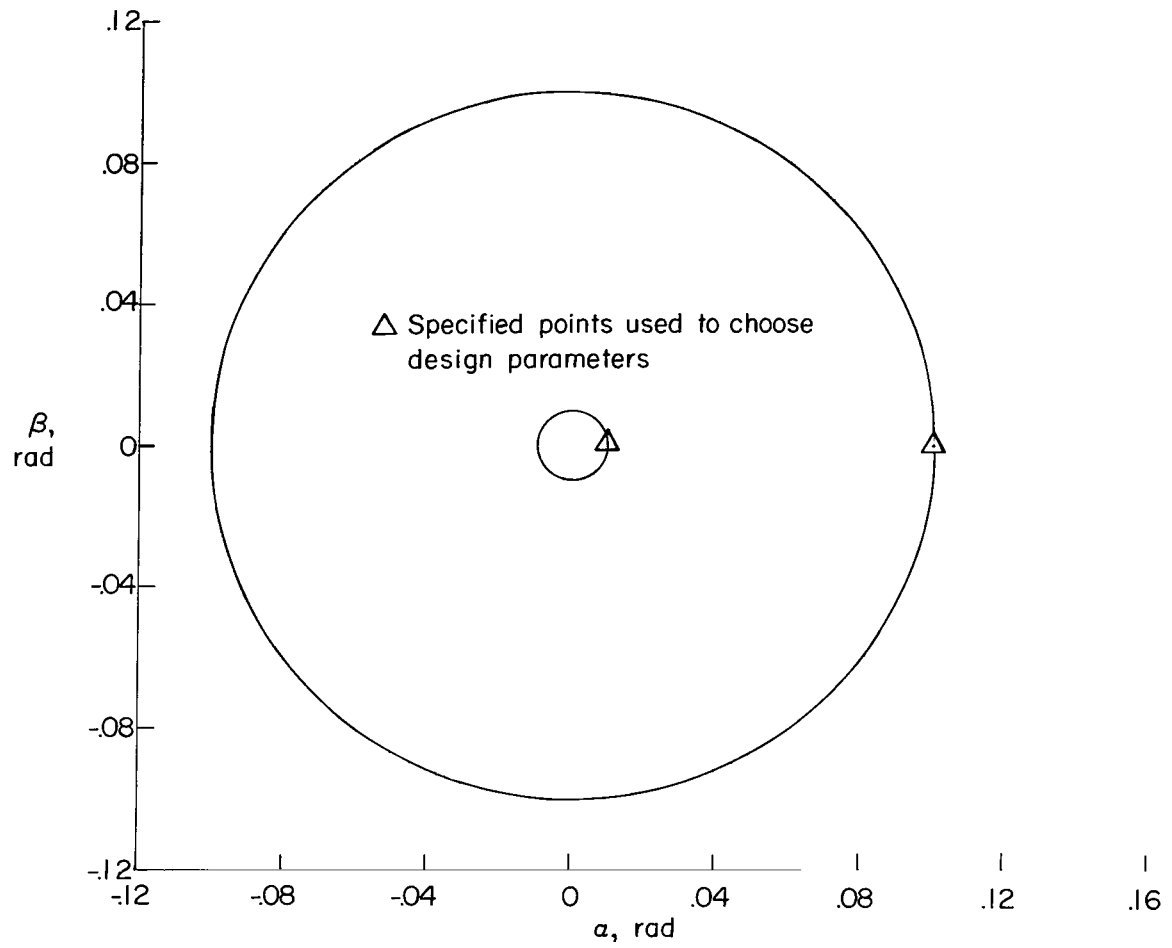
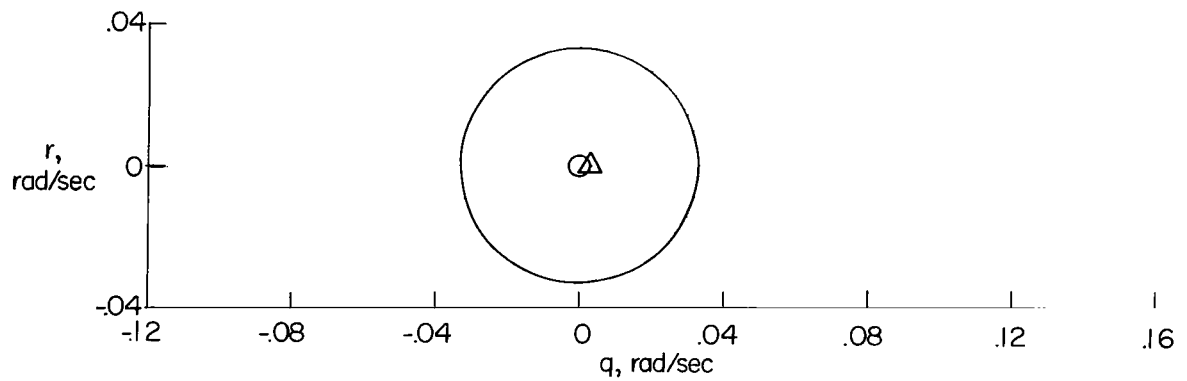


Figure 1.- Spinning space station.

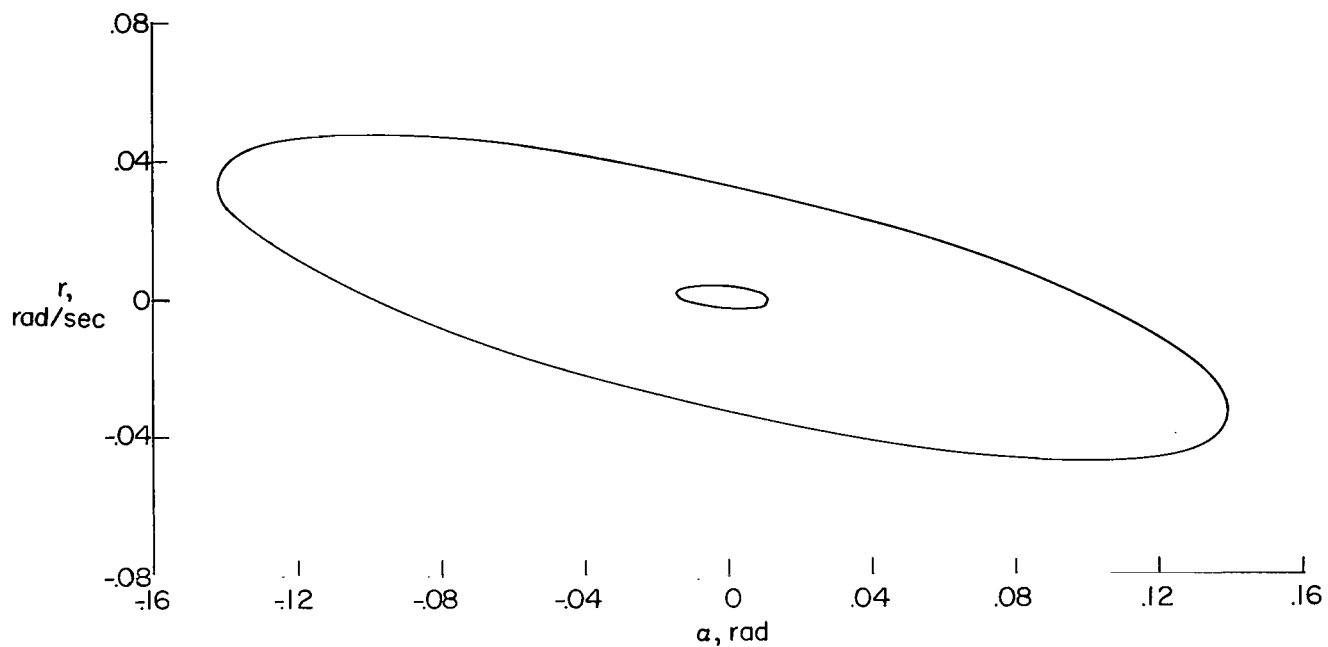


(a) Cross section in the $\alpha\beta$ -plane. $q = 0$; $r = 0$.

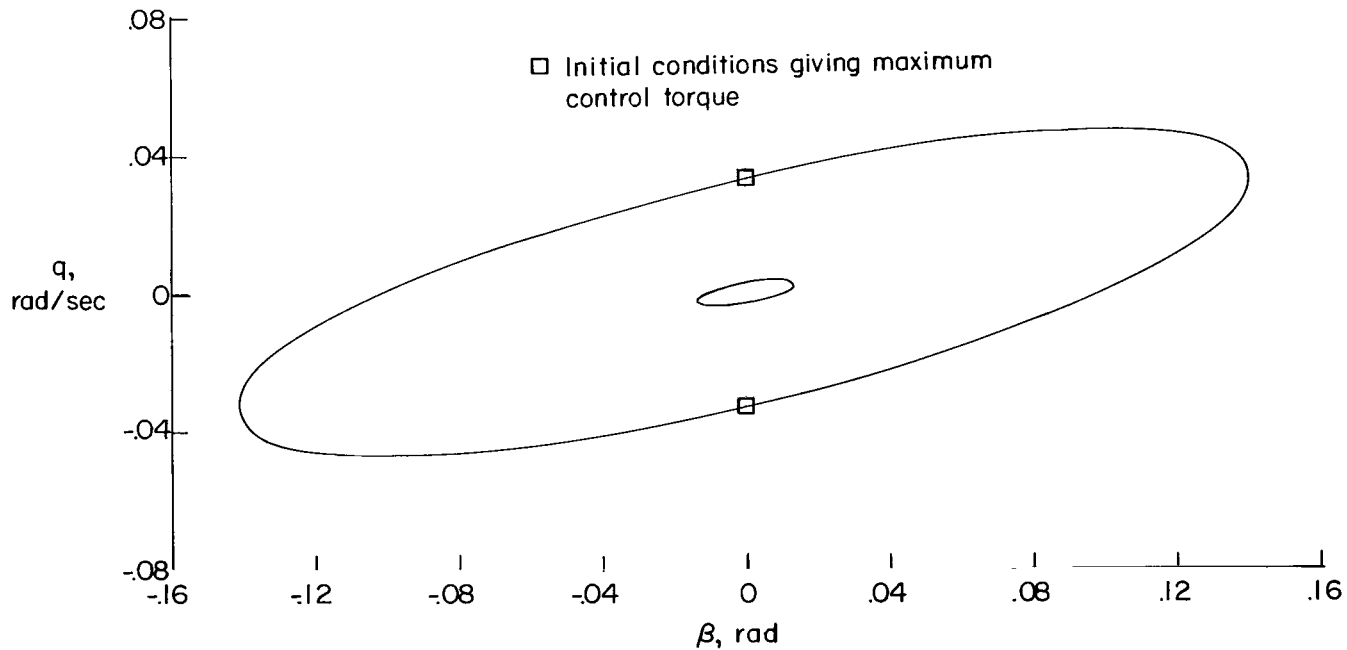


(b) Cross section in the qr -plane. $\alpha = 0$; $\beta = 0$.

Figure 2.- Cross sections of the inner and outer hyperellipsoids.



(c) Cross section in the α -plane. $q = 0$; $\beta = 0$.



(d) Cross section in the $q\beta$ -plane. $r = 0$; $\alpha = 0$.

Figure 2.- Concluded.

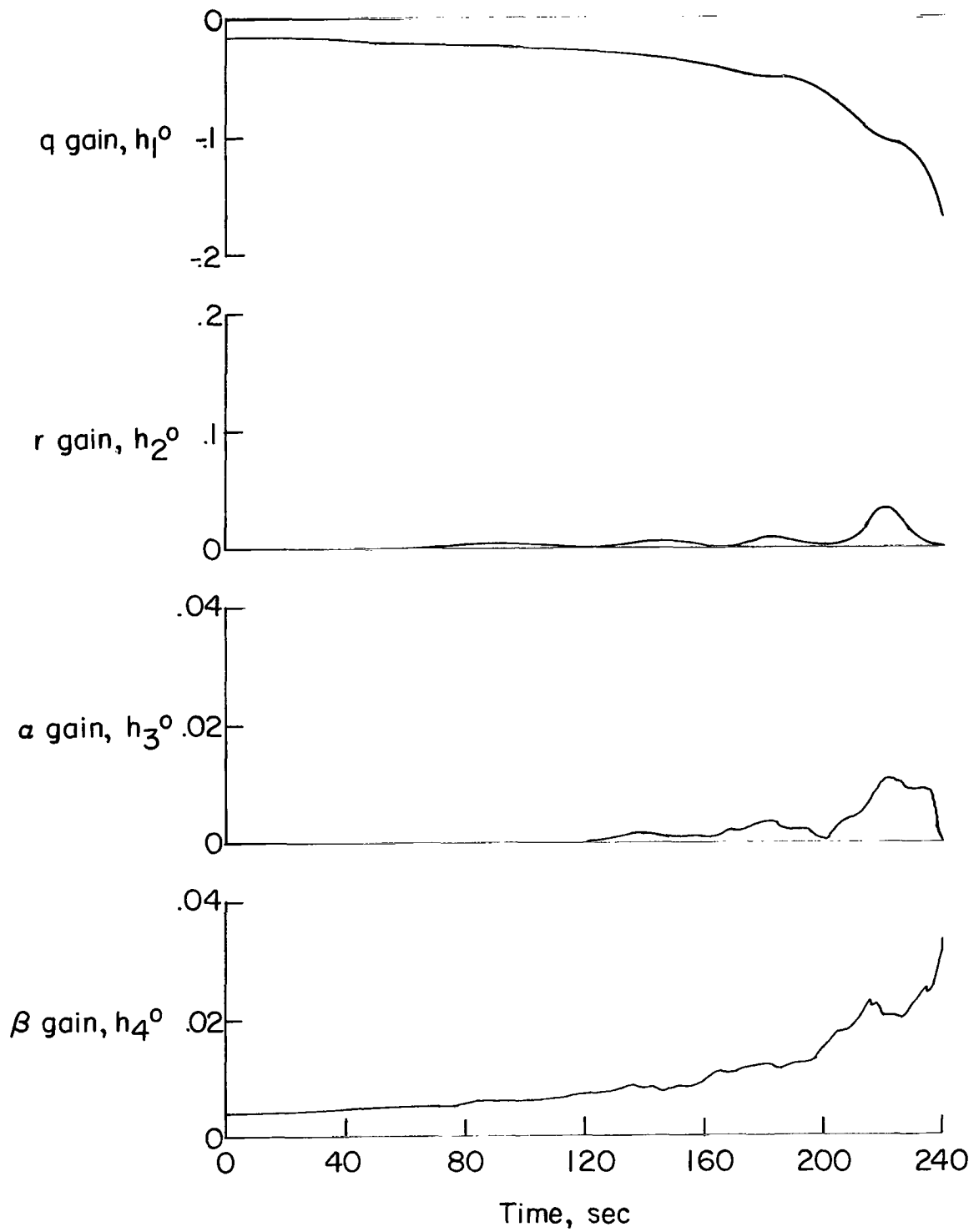


Figure 3.- Time-varying optimal gains.

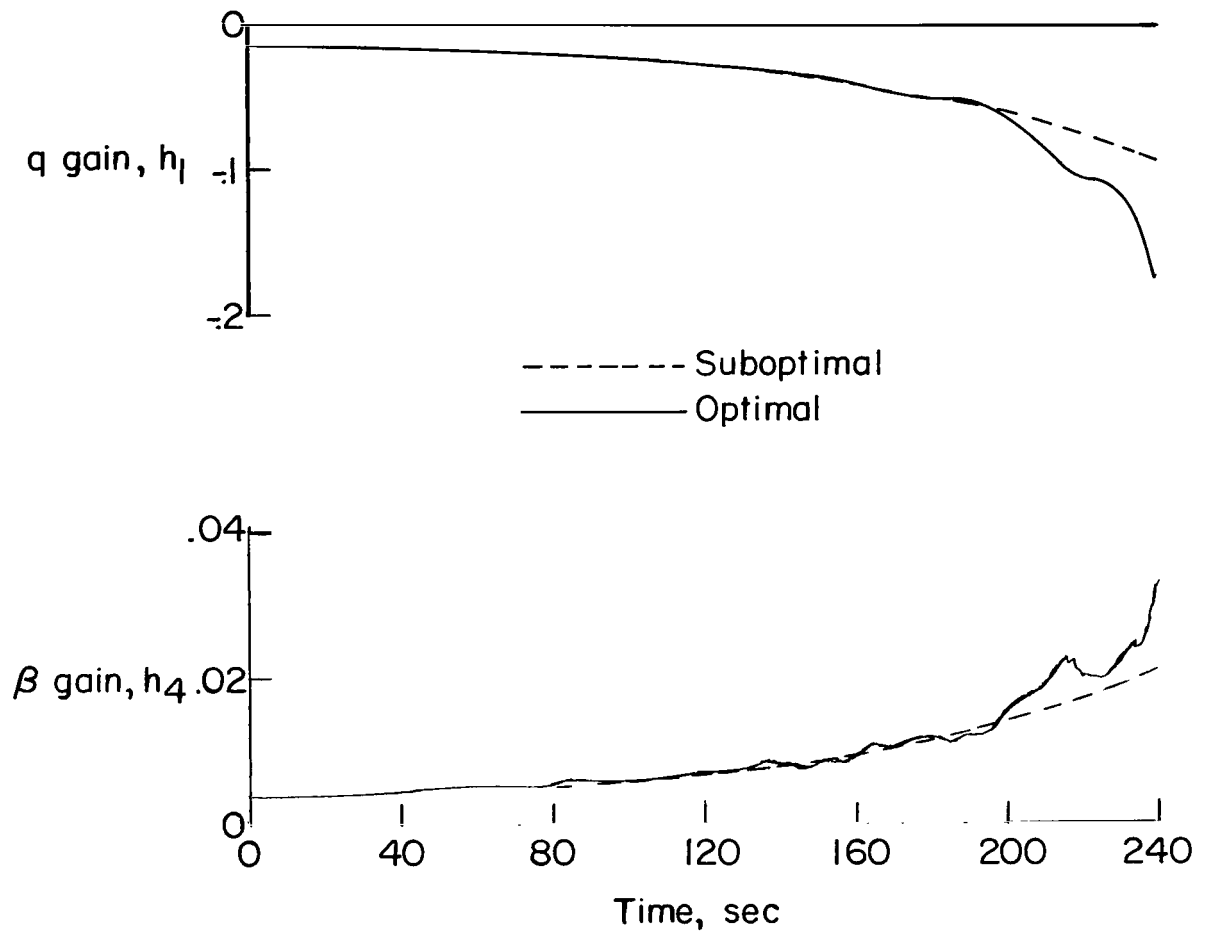


Figure 4.- Nonzero suboptimal gains compared with the optimal gains.

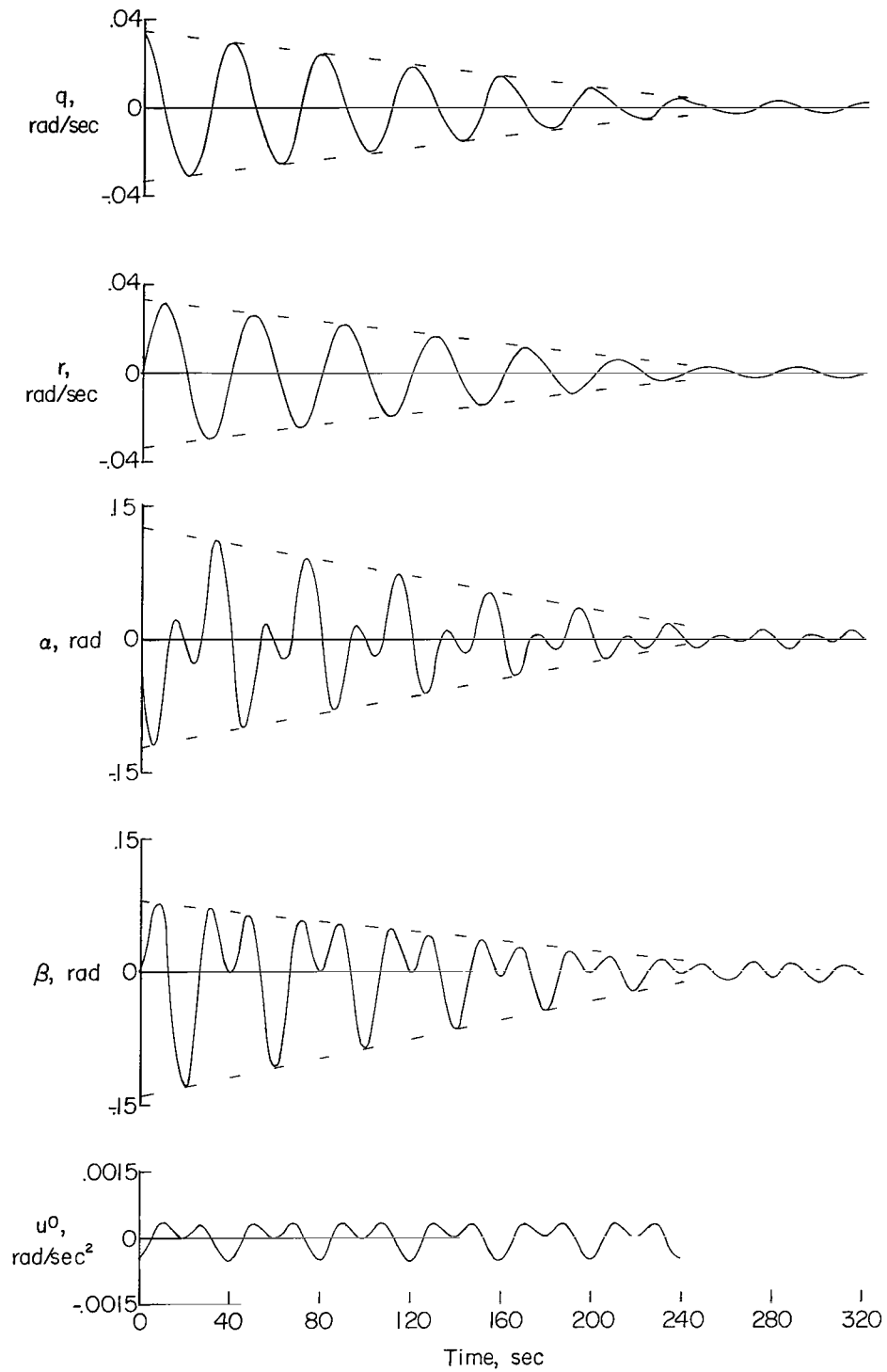


Figure 5.- Behavior of optimal regulator operating from the initial condition $q = 0.033$, $r = 0$, $\alpha = 0$, $\beta = 0$.

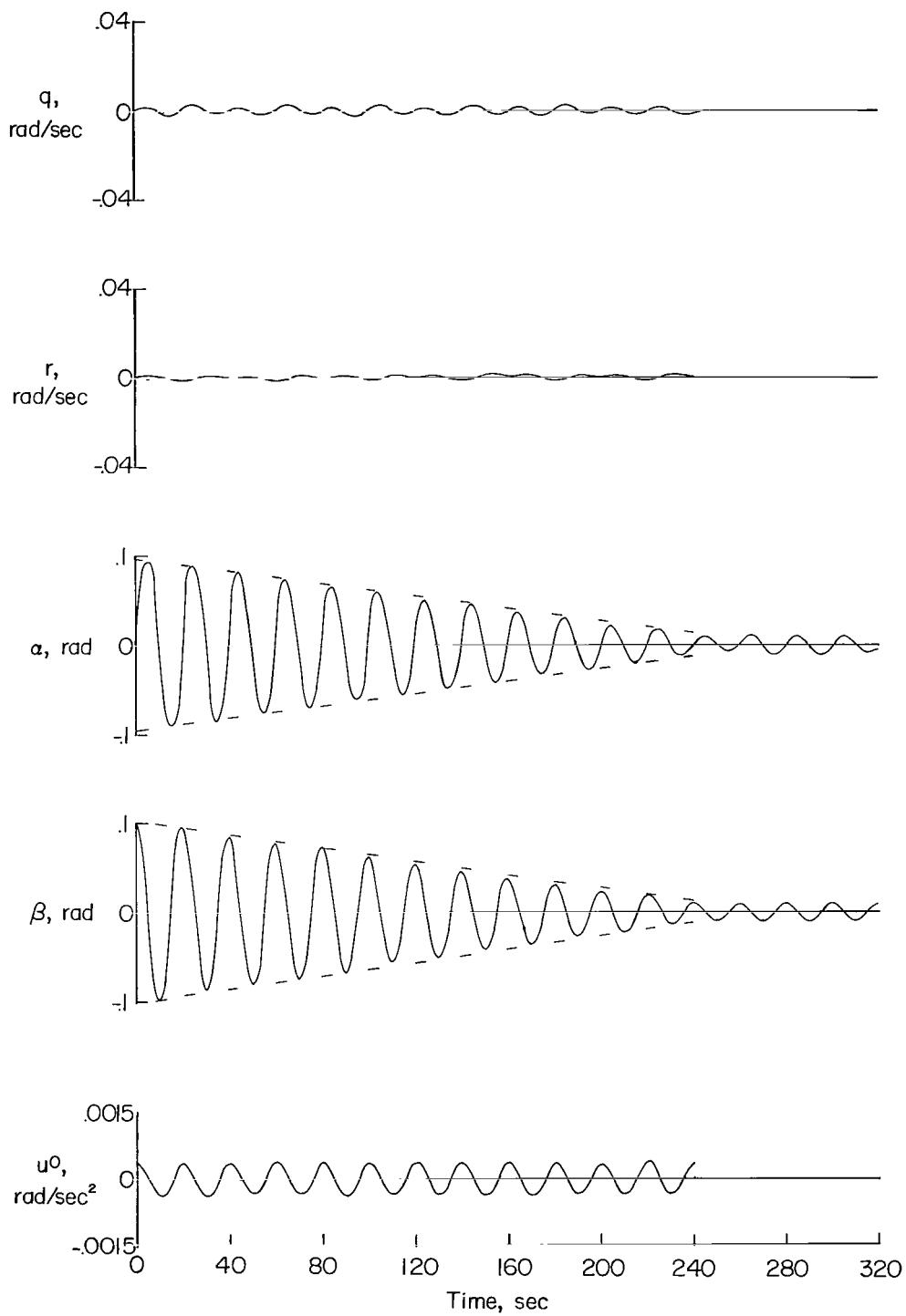


Figure 6.- Behavior of optimal regulator operating from the initial condition $\beta = 0.1$, $q = 0$, $r = 0$, $\alpha = 0$.

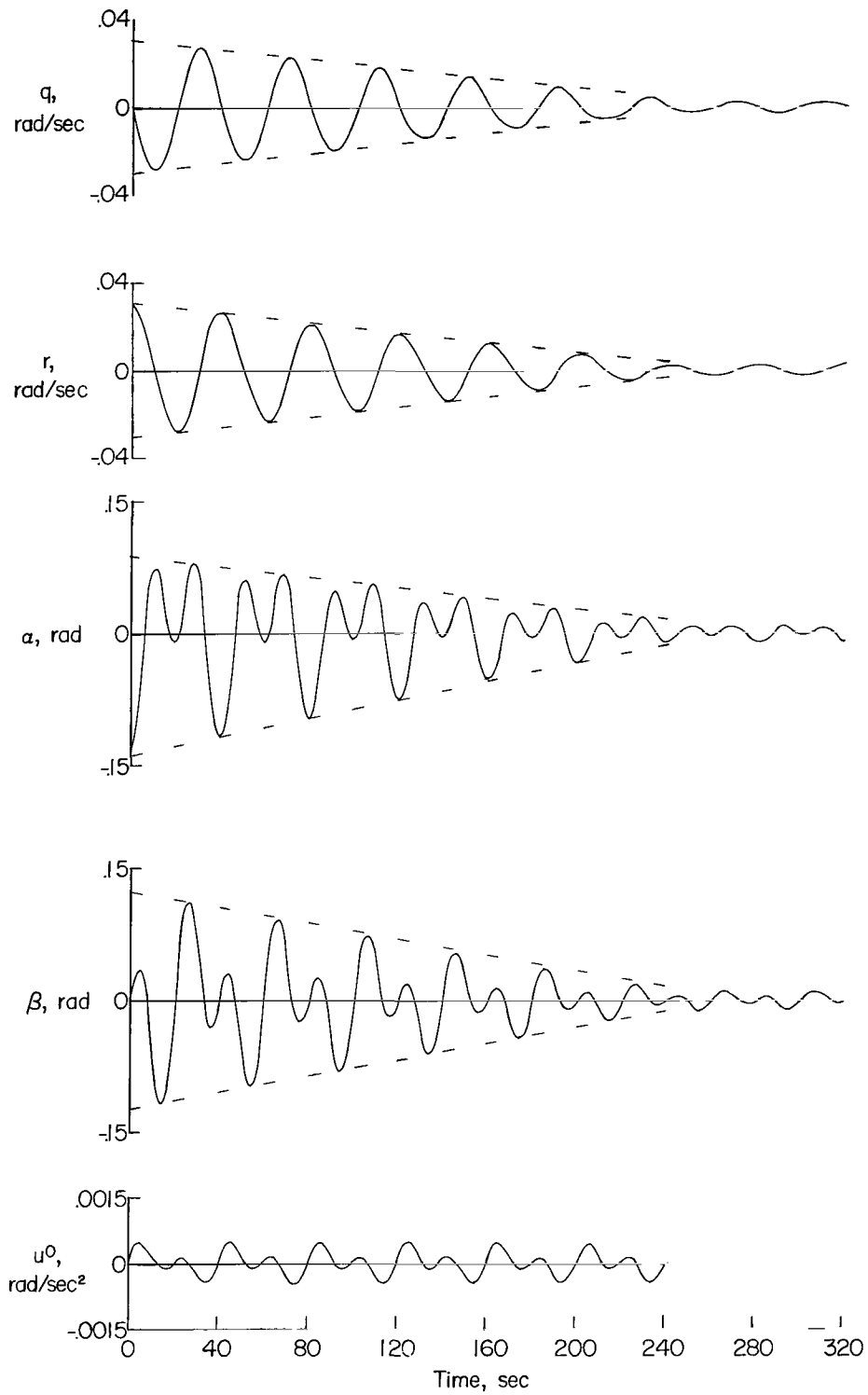


Figure 7.- Behavior of optimal regulator operating from the initial condition $r = 0.033$, $\alpha = -0.141$, $q = 0$, $\beta = 0$.

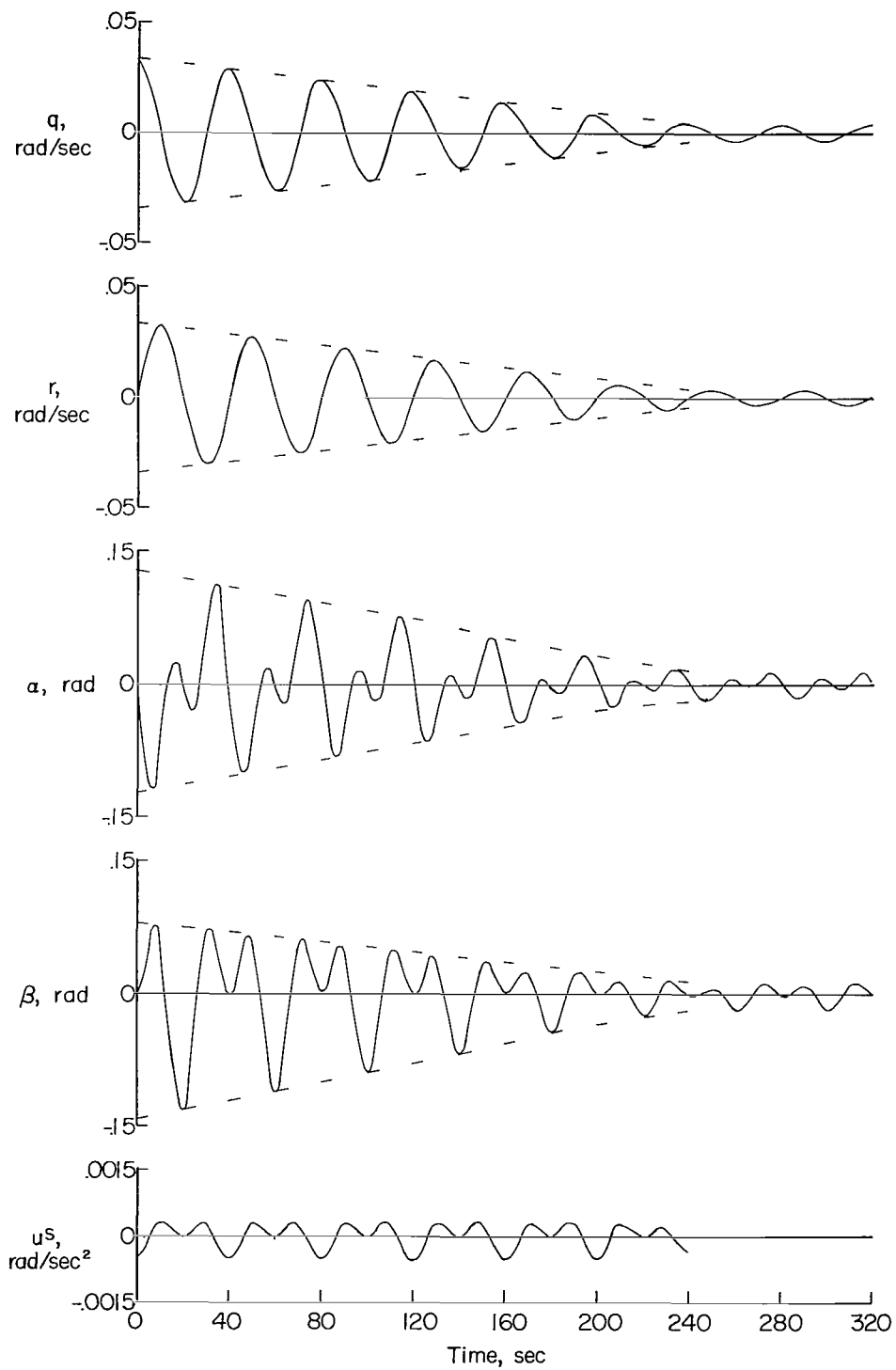


Figure 8.- Behavior of suboptimal regulator operating from the initial condition $q \approx 0.033$, $r = 0$, $\alpha = 0$, $\beta = 0$.

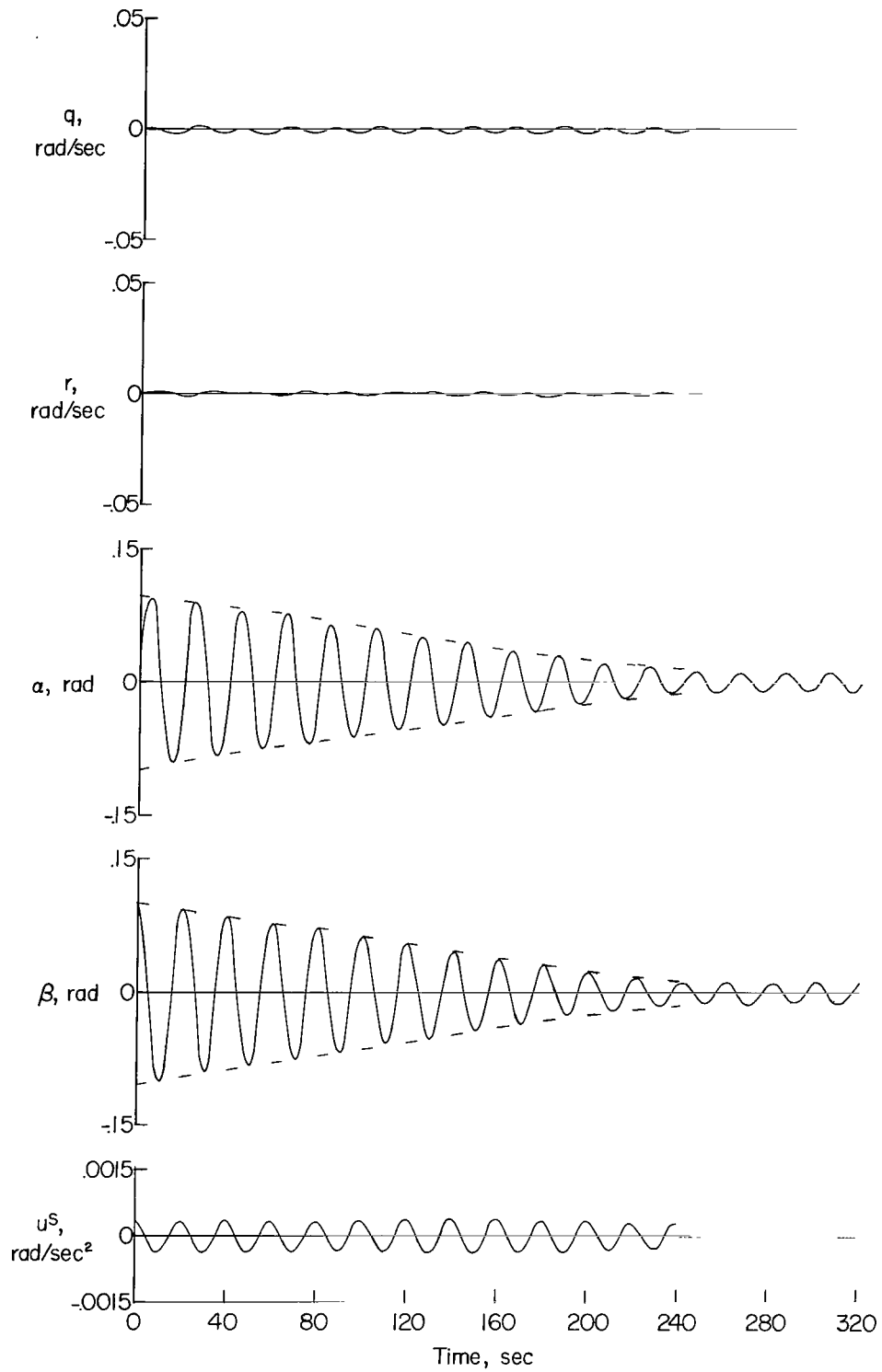


Figure 9.- Behavior of suboptimal regulator operating from the initial condition $\beta = 0.1$, $q = 0$, $r = 0$, $\alpha = 0$.

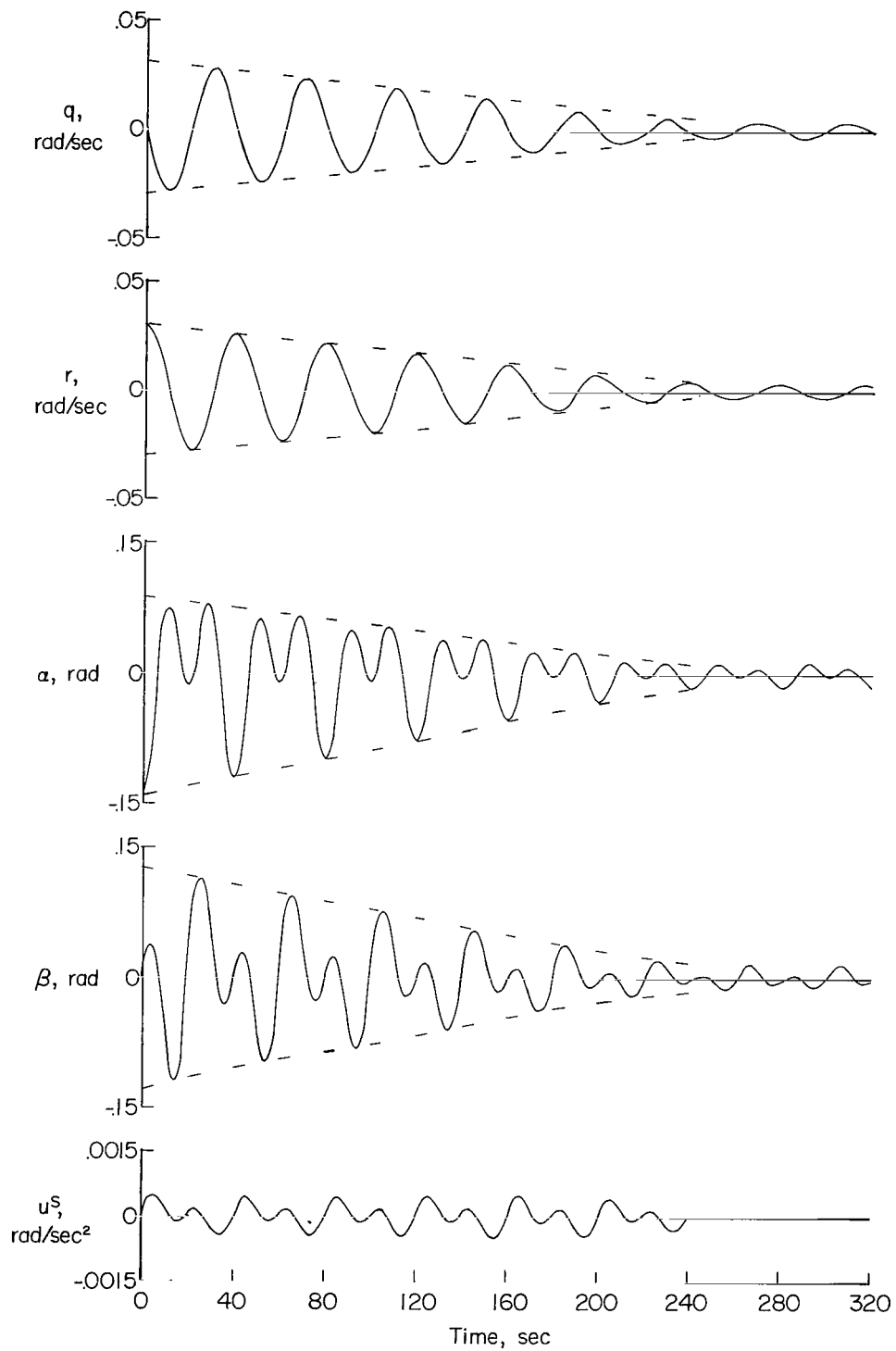


Figure 10.- Behavior of suboptimal regulator operating from the initial condition $r = 0.033$, $\alpha = -0.141$, $q = 0$, $\beta = 0$.

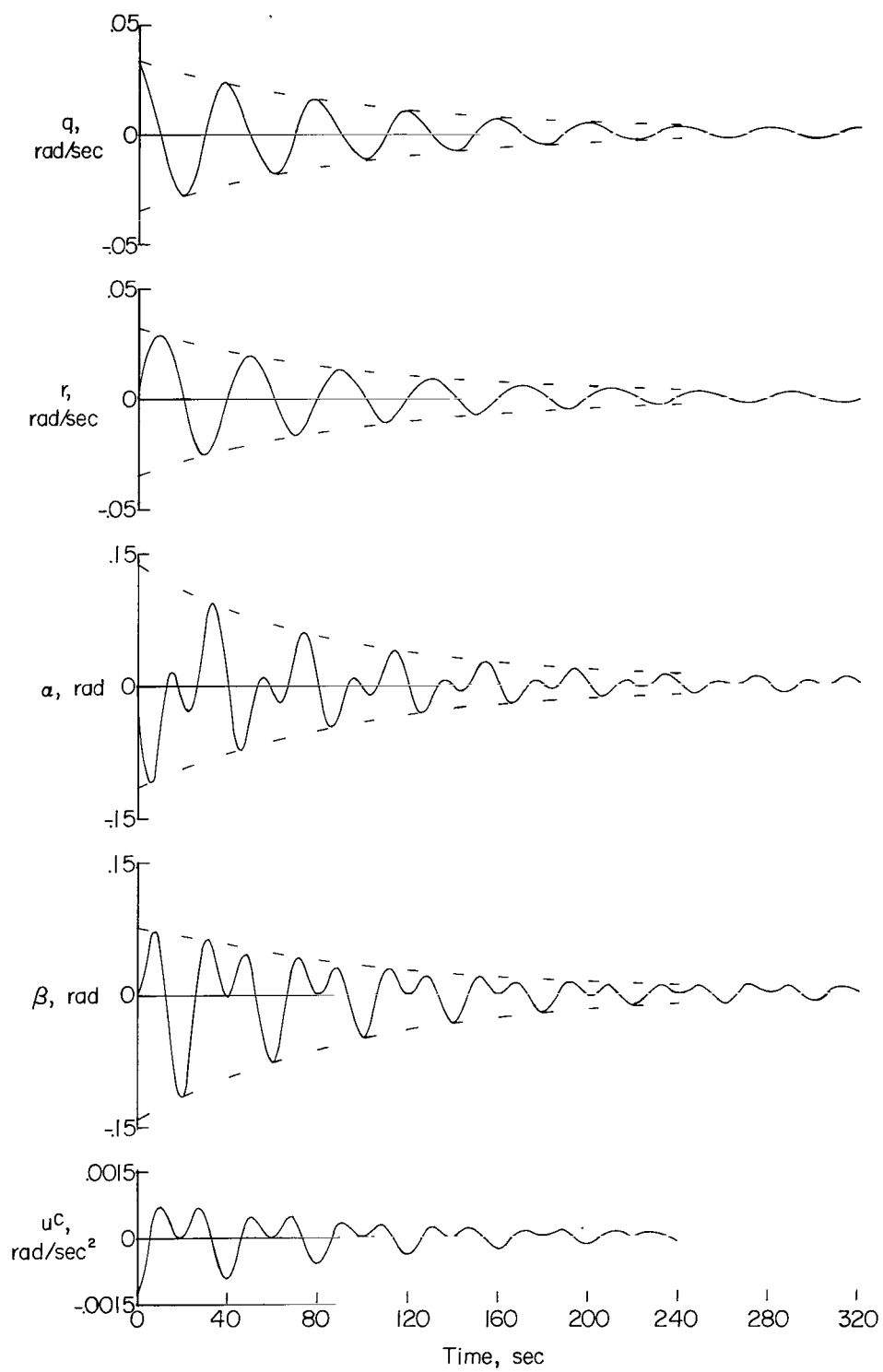


Figure 11.- Behavior of constant-gain regulator operating from the initial condition $q = 0.033$, $r = 0$, $\alpha = 0$, $\beta = 0$.

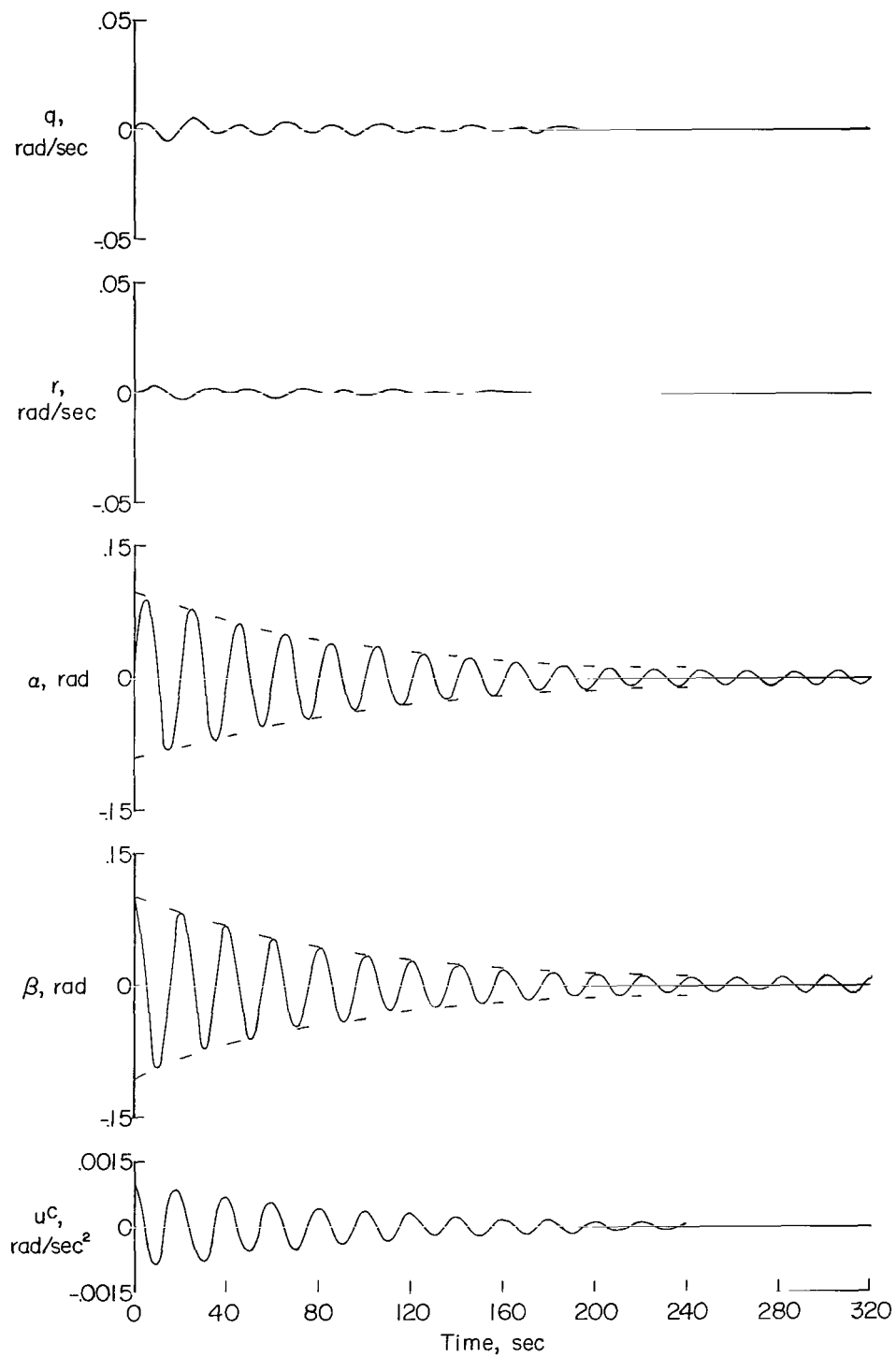


Figure 12.- Behavior of the constant-gain regulator operating from the initial condition $\beta = 0.1$, $q = 0$, $r = 0$, $\alpha = 0$.

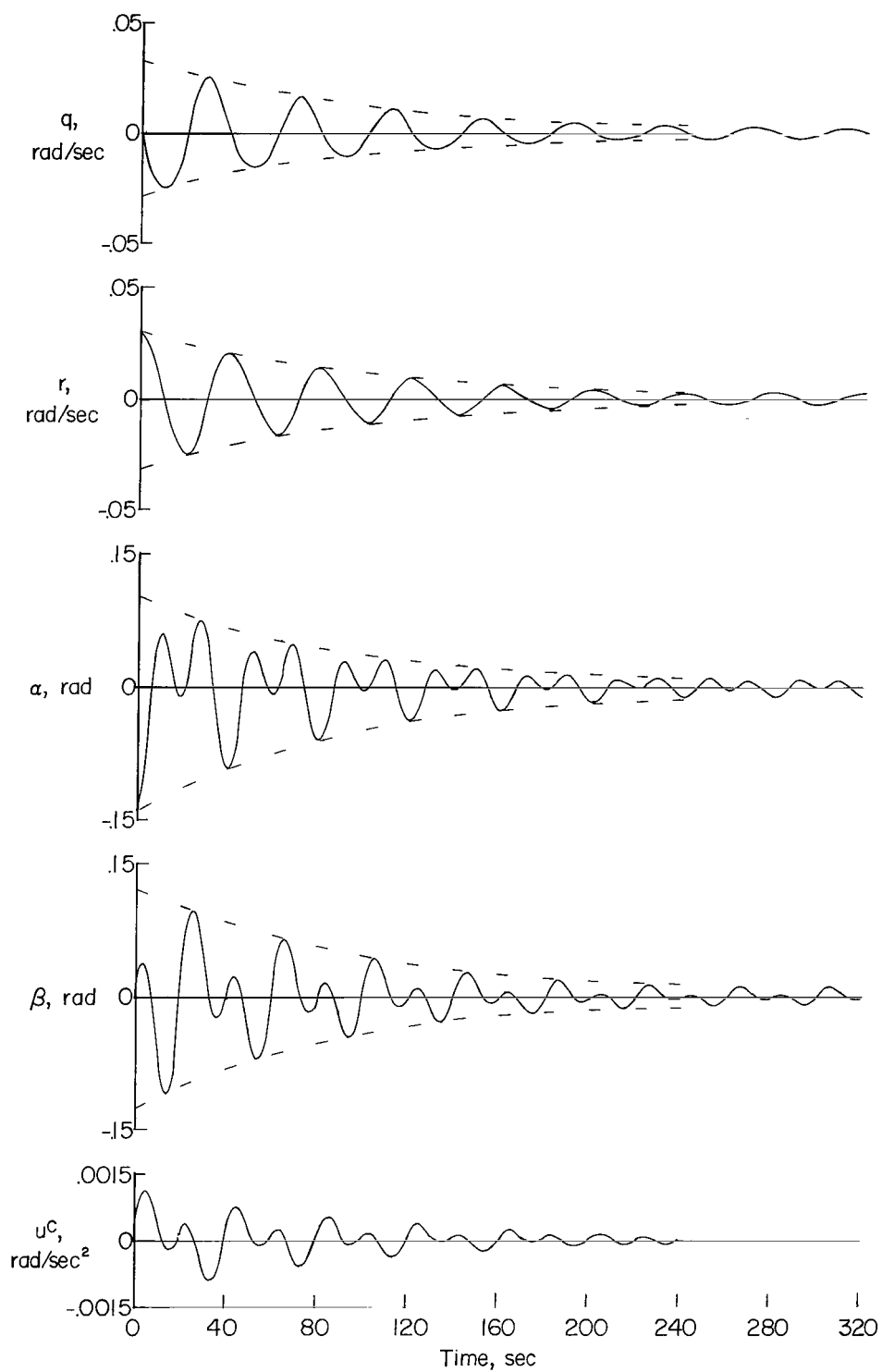


Figure 13.- Behavior of the constant-gain regulator operating from the initial condition $r = 0.033$, $\alpha = -0.141$, $q = 0$, $\beta = 0$.

"The aeronautical and space activities of the United States shall be conducted so as to contribute . . . to the expansion of human knowledge of phenomena in the atmosphere and space. The Administration shall provide for the widest practicable and appropriate dissemination of information concerning its activities and the results thereof."

—NATIONAL AERONAUTICS AND SPACE ACT OF 1958

NASA SCIENTIFIC AND TECHNICAL PUBLICATIONS

TECHNICAL REPORTS: Scientific and technical information considered important, complete, and a lasting contribution to existing knowledge.

TECHNICAL NOTES: Information less broad in scope but nevertheless of importance as a contribution to existing knowledge.

TECHNICAL MEMORANDUMS: Information receiving limited distribution because of preliminary data, security classification, or other reasons.

CONTRACTOR REPORTS: Technical information generated in connection with a NASA contract or grant and released under NASA auspices.

TECHNICAL TRANSLATIONS: Information published in a foreign language considered to merit NASA distribution in English.

TECHNICAL REPRINTS: Information derived from NASA activities and initially published in the form of journal articles.

SPECIAL PUBLICATIONS: Information derived from or of value to NASA activities but not necessarily reporting the results of individual NASA-programmed scientific efforts. Publications include conference proceedings, monographs, data compilations, handbooks, sourcebooks, and special bibliographies.

Details on the availability of these publications may be obtained from:

SCIENTIFIC AND TECHNICAL INFORMATION DIVISION
NATIONAL AERONAUTICS AND SPACE ADMINISTRATION
Washington, D.C. 20546